

High resolution strain measurements in highly disordered materials

Mark Sutton

Physics Department, McGill University, Montréal, Quebec H3A 2T8, Canada

J.R.M. Lhermitte

*Center for Functional Nanomaterials,
Brookhaven National Laboratory, Upton, New York 11973 US*

Françoise Ehrburger-Dolle

Univ. Grenoble 1 / CNRS, LIPhy UMR 5588, Grenoble, F-38041, France

Frédéric Livet

*SIMaP, Grenoble INP-CNRS-UJF, BP. 75,
38402 Saint Martin dHères cedex, France*

Abstract

The ability to measure small deformations or strains is useful for understanding many aspects of materials. Here, a new analysis of speckle diffraction peaks is presented in which the systematic shifts of the speckles are analyzed allowing for strain (or flow) patterns to be inferred. This speckle tracking technique measures strain patterns with a accuracy similar to x-ray single crystal measurements but in amorphous or highly disordered materials.

PACS numbers:

The measurement of small deformations in samples is a useful method to characterize the properties of materials, soft materials in particular. Deformations are typically measured via strain, or the geometrical relative displacements of elements in a body. High resolution strain has been measured using x-rays and neutron scattering ([1], [2], [3]) and visible light ([4], [5], [6]). However, these measurements were mostly limited to crystalline materials and or macroscopic sections of samples. There are few measurement techniques involving amorphous materials with x-rays. The Nielsen group [3] applied a 3D absorption tomography technique. This technique provides a high resolution 3 dimensional picture of the static strain of materials. However, scan times are long, with at least 2 hours per scan. The long times make it difficult for in-situ measurements, where the strain may occur over short times. In this paper a technique using XPCS is proposed for in-situ measurements of strain in amorphous materials.

For a simple insight into the technique, imagine a deformation of the underlying space, $\vec{r}' = M \cdot \vec{r}$. For small deformations, the transformation consists of a possible rigid body displacement and a local distortion, $\nabla \cdot M$. From this it follows that the strain is the difference between $\nabla \cdot M$ and the identity matrix. When $\nabla \cdot M$ is independent of \vec{r} a homogeneous deformation results. Consider the effect on the density, $\rho(\vec{r})$, and its Fourier transform, $\rho(\vec{Q})$. To get the Fourier transform of the deformed material, $\rho'(\vec{Q})$:

$$\begin{aligned}\rho'(\vec{Q}) &= \int \rho(M \cdot \vec{r}) e^{-i\vec{Q} \cdot \vec{r}} d\vec{r} \\ &= \rho(M^{-T} \cdot \vec{Q}) / \det(M),\end{aligned}$$

by simple substitution. This calculation assumes a negligible change in the volume of integration. Speckle measurements use a small diffraction volume and this sets the scale determining when a deformation is small and for which the approximation is to be valid. Another approach is given by solving the convection-advection diffusion equation by the method of characteristics and may be found in Fuller et. al [7]. So, if we can relate features in $\rho(\vec{q})$ (or scattering intensity) before and after the deformation, their time dependent shifts in reciprocal space are:

$$\begin{aligned}\frac{\Delta(\vec{Q} - M^T \cdot \vec{Q})}{dt} &= \\ \frac{d\vec{Q}}{dt} &= -\Gamma^T \cdot \vec{Q}\end{aligned}$$

and related to the transpose of the deformation. For a simple velocity field

$$M(t) \cdot \vec{r} = \int_0^t \vec{v}(\vec{r}, \tau) d\tau = (\vec{v}_0 + \Gamma \cdot \vec{r})t + \vec{r}.$$

The deformation gradient tensor is related to the velocity gradient matrix, $\Gamma = \nabla \vec{v}(\vec{r})$ for a velocity field. The rigid body shift gives a phase factor, $\exp(i\vec{v}_0 \cdot \vec{Q}\tau)$, due to the shift in \vec{r} and has been ignored as it will not be seen in the scattered intensity.

The related wave-vector for a deformation can be obtained from the following correlation function:

$$g_2(\vec{Q}_0, \Delta\vec{Q}, \tau) = \frac{\langle I(\vec{Q}, t) I(\vec{Q} + \Delta\vec{Q}, t + \tau) \rangle_{\vec{Q}}}{\bar{I}^2}$$

where the average is over a small region in \vec{Q} centered around \vec{Q}_0 . Noticing that when the shifts are time invariant, it is possible to also average in time. This correlation function is an extension of the intensity-intensity correlation function used in XPCS, where $\Delta\vec{Q} = 0$. When the scattering is sharply peaked, as for Bragg peaks and for speckles in coherent diffraction, one measures $\Delta\vec{Q}$ by following the local maxima.

The experiments were carried out at beamline 8-ID-I of the Advanced Photon Source. For this setup, the energy was 7.35 Kev ($\lambda = 1.67 \text{ \AA}$) monochromated by double bounce Ge(111) crystals. The incident flux was $\approx 10^9$ photons/sec through a $20 \times 20 \mu\text{m}^2$ aperture. Each pixel in the area detector corresponds to $2.0 \times 10^{-5} \text{ \AA}^{-1}$, which is close to the speckle size. The filled rubber samples were held in a vacuum chamber with an in-situ tensile stress-strain cell. The exposure time per frame was .1 second recurring every 2.0 seconds. Further details are given in references [8, 9].

The sample consists of a cross-linked elastomer (Ethylene Propylene Diene Monomer, EPDM, rubber) filled with hydroxylated pyrogenic silica (Aerosil 200 [10–12]). The volume fraction of silica is close to 0.16. In our measurements, the one millimeter thick sheets are punched out to a classical dumb-bell shape (width = 4 mm). As described in Ref. [8] upon applying a step strain on the sample, the stress jumps and then slowly relaxes as the sample is held at constant strain. For this article, only one 400 second data set is presented for a sample which was stretched by 60%. The data collection for this run started approximately 1250 seconds after the application of the strain step. This data is part of those in Ref. [8]. A single run is described as this simplifies the exposition of the technique. The description of the rheological aspects of the measurements is partially described in the references [8, 9]. The implications of this new analysis on the viscoelastic properties of the various samples is left for a future paper.

To calculate the cross-correlations, the scattering images were decomposed into wedges or bins of ΔQ and $\Delta\phi$. The azimuthal angle ϕ is oriented with increasing horizontal pixels from beam

center as 0° . The orientation of the detector is such that up on an image is up in the sample. The wedges are 20 pixels ($.001 \text{ \AA}^{-1}$) wide in $|\vec{Q}|$ and 10° in ϕ . Cross-correlations for all wedges with more than 1000 pixels up to wave-vector $.024 \text{ \AA}^{-1}$ (1200 pixels) were calculated. This gave 376 wedges. Bins are numbered with ϕ increasing for fixed Q and then Q increases for the next set of ϕ . Figure 1 shows a typical bin, bin 57 and its cross-correlation. As for each cross-correlation [13, 14] it has a peak of size $1 + \beta$ (speckle contrast) sitting on a background of one. Each cross-correlation is least squares fit to a 2D Gaussian peak with widths giving the speckle size. The shift of the peak from the center gives the speckle movement. Figure 1c demonstrates that it is easy to see a shift by a fraction of a pixel as reflected by the asymmetric placement of the data around the center. A preliminary version of this analysis is given in Lhermitte's PhD thesis [15].

Figure 2 shows a representation of the speckle shifts between two selected times. The intensity of the time averaged small angle scattering is plotted underneath. The shift for each bin is plotted as an arrow starting at the center of the bin. Since the shifts are so small the shift in pixels has been multiplied by 10. One can immediately see that the relaxation of the filled rubber has a hyperbolic flow pattern. It is away from the beam center in vertical ($\phi = 270^\circ$) and towards the beam center in the horizontal ($\phi = 180^\circ$). One also sees the shift increases with $|\vec{Q}|$.

Figure 3 shows the $g_2(\tau)$, as one would calculate it in a XPCS measurement. The slower decaying line in Fig. 3 is obtained by following the peak shift $\Delta\vec{Q}$ [16]. The decay time observed is the time it takes for a speckle to move through three dimensional reciprocal space. Given the expected uniaxial like nature of the strain, we expect the time for the speckle to move perpendicular to the detector plane to be comparable for the time of in-plane motion. It is this speckle motion that leads to the time constants varying as q^{-1} observed in Ref. [8]. The small angle x-ray scattering (SAXS) with the speckle averaged away is equivalent to a conventional SAXS measurement and this did not vary during the course of these measurements.

A cross-correlation can be calculated for each bin and each pair of diffraction patterns. Single frame cross-correlations give quite acceptable correlations but for this analysis 5 images are first averaged and then correlated to get cleaner correlations. Since the correlations die away in approximately 50 seconds, the shifts are measured by cross-correlating each nearest time pair of the averaged scattering. Summing the shifts leads to a cumulative shift over the run and is shown in Fig. 4 for bin 57. For a given time and from the cumulative shifts in each bin, a vector field may be calculated. Two examples of these are plotted in Fig. 2. For each delay time slice the vector field can be fit by: $d\vec{Q}/dt = -\Gamma \cdot \vec{Q}$ where $d\vec{Q}$ comes from the measured shifts and dt is the time

between images. The 2D matrix Γ is diagonal and such a fit is shown in Fig. 5. This simple two parameter fit, fits all Q - ϕ bins exceptionally well for each time pair.

Figure 6 shows the evolution of the diagonal elements of Γ as a function of time obtained from all vector field fits. A value of $\Gamma = .000035$ per second corresponds to a maximum spread in velocities of $\approx 170 \text{ \AA}/\text{sec}$ across $5 \mu\text{m}$ perpendicular to the incident beam. The evolution of Γ with time reflects the slow visco-elastic relaxation in the rubber.

In conclusion, it has been shown that a simple extension of XPCS can measure the projection of the velocity field across the scattering volume. Since the dimensions of the beam are $20 \times 20 \mu\text{m}^2$ this gives a submicron measurement of the local strain fields and the strain precision is similar to or better than what can be measured in a single crystal. It is stressed here that this analysis works for amorphous or highly disordered materials, in particular most heterogeneous soft matter systems. Details of the rheological implications for our samples and for the conventional XPCS analysis [17] from this new approach is left for future articles.

Nothing in the above analysis is specific to elastomers except maybe for the uniaxial approximation used to fit the vector field. Other distortions may need a different model. It should also be noted that the strain measurements only required two images with sufficient intensity to measure their speckle patterns and that the two images are separated in time by less than the time it takes for a speckle to move out of the beam. The advent of the new lattice structures that are being used to upgrade the x-ray synchrotrons will lead to an increase in coherence by two to three orders of magnitude. These kinds of measurements should be able to be pushed to give at least microsecond time resolution.

This research used resources of the Advanced Photon Source, a U.S. Department of Energy (DOE) Office of Science User Facility operated for the DOE Office of Science by Argonne National Laboratory under Contract No. DE-AC02-06CH11357. We thank the staff of beamline 8-ID-I for their excellent help.

[1] I. Robinson and R. Harder, *Nature materials*, **8**, 291–298, (2009).

[2] A.J. Allen, M.T. Hutchings, C.G. Windsor, and C. Andreani, *Advances in Physics*, **34**, 445–473, (1985).

[3] S.F. Nielsen, H. F. Poulsen, F. Beckmann, C. Thorning, and J.A. Wert, *Acta Materialia*, **51**, 2407–

- 2415, (2003).
- [4] T.C. Chu, W.F. Ranson, and M.A. Sutton, *Experimental mechanics*, **25**, 232–244, (1985).
- [5] M.A. Sutton, W.J. Wolters, W.H. Peters, W.F. Ranson, and S.R. McNeill, *Image and Vision Computing*, **1**, 133–139, (1983).
- [6] I. Yamaguchi, *Journal of Physics E: Scientific Instruments*, **14**, 1270, (1981).
- [7] G.G. Fuller, J.M. Rallison, R.L. Schmidt, and L.G. Leal. *Journal of Fluid Mechanics*, **100**, 555–575, (1980).
- [8] F. Ehrburger-Dolle, I. Morfin, F. Bley, F. Livet, G. Heinrich, S. Richter, L. Piché, and M. Sutton, *Macromolecules*, **45**, 8691-8701 (2012).
- [9] F. Ehrburger-Dolle, I. Morfin, F. Bley, F. Livet, G. Heinrich, L. Piché, and M. Sutton, *Journal of Polymer Science Part B: Polymer Physics* **52**, 647-656, (2014).
- [10] T.P. Rieker, M. Hindermann-Bischoff, F. Ehrburger-Dolle, *Langmuir*, **16**, 5588-5592, (2000).
- [11] F. Ehrburger-Dolle, M. Hindermann-Bischoff, E. Geissler, C. Rochas, F. Bley, F. Livet, *Materials Research Society Symposium*, **661**, KK7.4.1, (2001).
- [12] F. Ehrburger-Dolle, F. Bley, E. Geissler, F. Livet, I. Morfin, C. Rochas, *Macromolecular Symposia*, **200**, 157–167, (2003).
- [13] Cross-correlations were calculated by taking each wedge and placing it in a rectangular matrix with a size of twice the tightest rectangle covering the wedge. Correlations were calculated using Fourier transforms by further extending the matrix to one with sizes that are multiples of 2,3 and 5. This insures the fast Fourier transform can be used. This rectangle has many zeros, including those outside the wedges and those due to bad or masked pixels. To take these into account, let B be a rectangular matrix of zeros and ones identifying which pixels have signal and I be the matrix of the same size with the signal to be correlated. Then $g_2 = ((I_0 \otimes I_1) \times (B \otimes B))/((B \otimes I_0) \times (I_1 \otimes B))$ where \times is element by element multiplication [14]. The denominator amounts to symmetric normalization.
- [14] D. Padfield, *IEEE Transactions on Image Processing*, **21**, 2706-2718, (2012)
- [15] J. Lhermitte, *Using Coherent Small Angle Xray Scattering to Measure Velocity Fields and Random Motion*. PhD thesis, McGill University, (2011).
- [16] The speckle shifted contrast was measured for the shifted peak by using the measured shift and interpolating the second image back to the position of the first, averaging the product of the two images and dividing by each average image.
- [17] F. Ehrburger-Dolle, I. Morfin, F. Bley, F. Livet, G. Heinrich, Y. Chushkin, and M. Sutton, *Soft Matter*

15, 3796-3806 (2019).

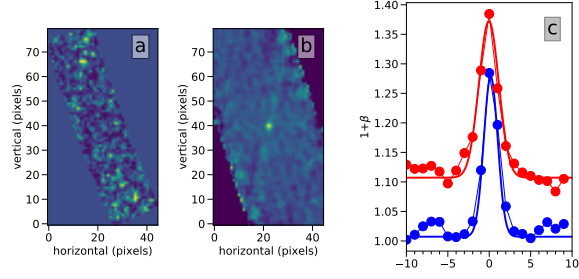


FIG. 1: a) Speckle intensity for bin 57, $q=0.009 \text{ \AA}^{-1}$, $\phi = 200^\circ$ as placed in a rectangular image. b) Cross-correlation between the first two averaged by 5 images. c) Line-outs along the central pixel of the cross-correlation in the vertical (red, offset in y by .1) and horizontal (blue) directions. The thick lines are for the 2D Gaussian that results from fitting the peak. The resulting shifts are .24 pixels in the horizontal and -.10 pixels in the vertical and reflected in the asymmetric placement of the measured points (dots) about zero.

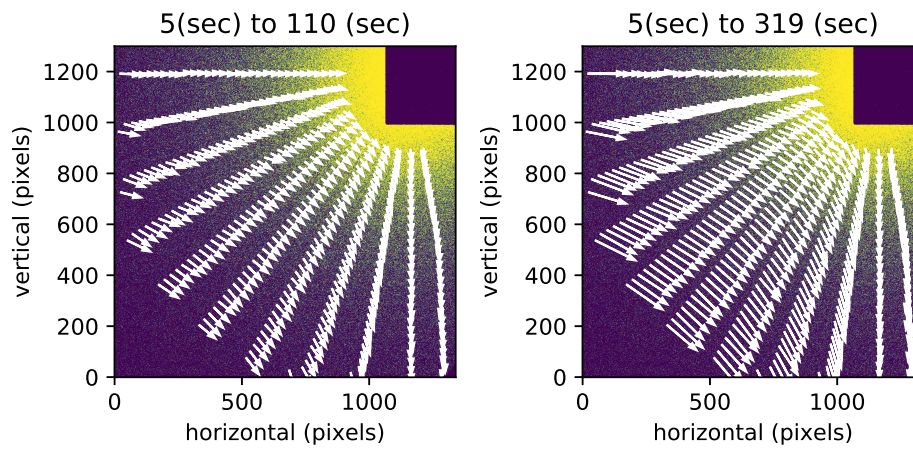


FIG. 2: Strain field for images from times 5 and 110 seconds and for images at 5 and 319 seconds. Each local Q region has a shift in the speckle pattern given by the arrows which are scaled up by 10 (Q per pixel = $2.00 \times 10^{-5} \text{ \AA}^{-1}$). The coordinates of the shifts for the right panel are plotted in Fig. 5. The shifts are superimposed on the underlying small angle x-ray scattering intensity.

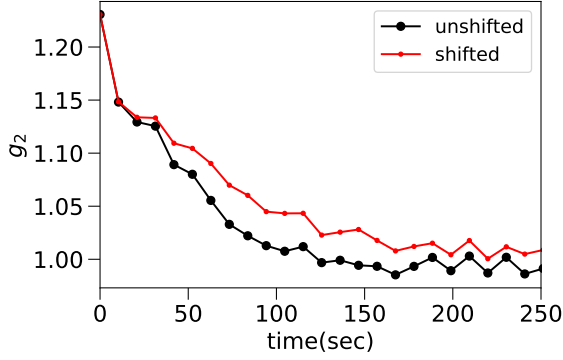


FIG. 3: Comparison of the conventional ($\Delta\vec{Q} = 0$) g_2 measurement to the one following the in-plane shift observed on the detector. This is the same Q - ϕ bin as Fig. 1.

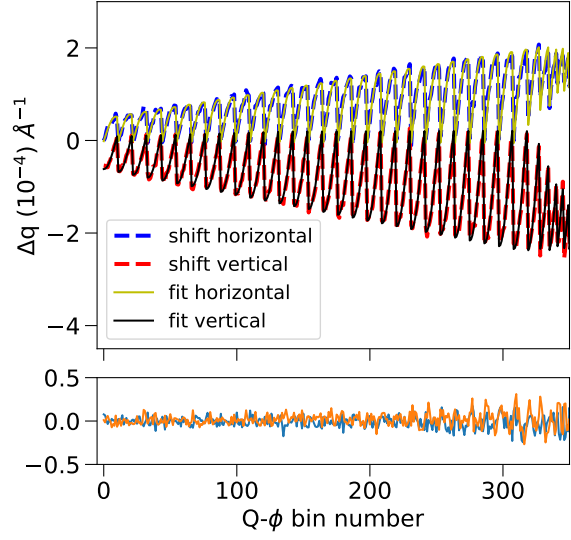


FIG. 5: Example of a two parameter fit to a simple diagonal deformation pattern. The fitted values overlap with the data and so the lower panel shows the two sets of differences. The vector field used in the fit is the same as one the right panel of Fig. 2 and corresponds to $\Gamma_{vert} = 31.97 \times 10^{-6}$ and $\Gamma_{hor} = -26.75 \times 10^{-6}$ per second. The Q - ϕ bin used in Figs [1,3 and 4] is bin 57.

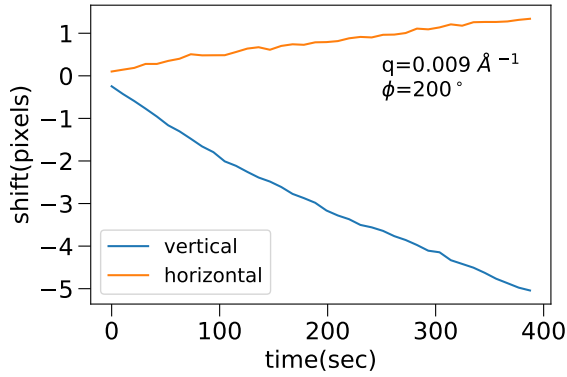


FIG. 4: The cumulative shift for bin 57 over the length of the time series.

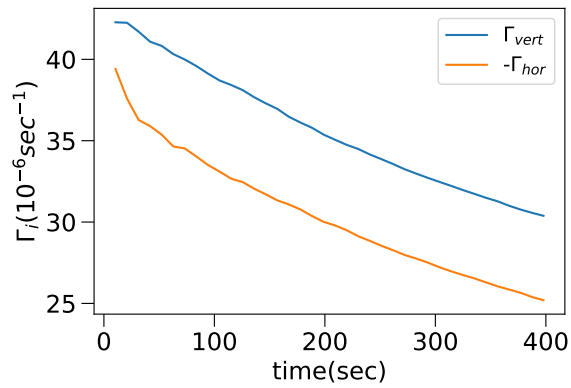


FIG. 6: Time evolution of the deformation parameters obtained by fitting the vector fields over the run.